Indian Journal of Engineering & Materials Sciences
Vol. 32, August 2025, pp. 447-461
DOI: 10.56042/ijems.v32i04.13284

Fully coupled analysis of a floating offshore wind turbine under wind and wave loading

Keerthana Mohan[a*] & Pabbisetty Harikrishna[a]

Wind Engineering Laboratory, CSIR-Structural Engineering Research Centre, Chennai – 600113, India

Received: 20 August 2024; accepted: 29 May 2025

Floating Offshore Wind Turbines (FOWTs) have been exposed to a multi-hazard scenario of wind and wave conditions, which have acted simultaneously. To assess their combined effect on the FOWT and to ensure the safety and stability of the supporting structure, numerous complex loading conditions such as wind-induced aerodynamic loads, wave-induced hydrodynamic loads, and the dynamics of the supporting structure have been considered. In this study, a comprehensive time-domain analysis of the NREL 5 MW Reference Wind Turbine (RWT) supported on the OC4 DeepCwind semi-submersible has been carried out under both operating and parked conditions using the aero-hydro-servo-elastic tool OpenFAST. The operating condition of the FOWT has included simulations at various wind speeds from cut-in to cut-out wind speed, with co-existing wave parameters for each wind speed. Based on the fully coupled analysis of the FOWT under simultaneously acting wind and wave conditions, the principal parameters required for the structural design of the rotor and supporting structure such as blade-root moments and tower fore-aft/overturning moments have been presented, alongside the key aspects of environment-structure interactions.

Keywords: Aerodynamics, Coupled analysis, Semi-submersible, Wind turbines

1 Introduction

Global transition to renewable energy sources from fossil fuels is evident from rapid increase in installed power capacity from wind and solar PV. By 2023, global renewable energy capacity stood at about 3,870 GW, with nearly 473 GW added during the year. The installations based wind energy are envisaged to quadruple by the end of decade to achieve net zero pathway[1]. Floating Offshore Wind Turbines (FOWT) have proven their merit as the next generation wind turbine technology owing to uninterrupted power generation potential from smoother wind characteristics in the ocean. Offshore wind turbines can either be fixed-bottom or floating, the key difference being the type of supporting structure. The type of supporting structure is decided mainly based on the water depth[2]. The nacelle movement is minimal/limited in case of fixed offshore and land based turbines. Significant fore-aft movement of nacelle makes the analysis of FOWT highly complex. The Levelized Cost of Energy (LCOE) for onshore wind power generation is $0.039/kWh, whereas that from offshore is $0.084/kWh[1]. Cost of offshore wind turbines are significantly higher than the onshore turbines. Thus, fewer numbers of turbines with higher rated capacities are adopted for offshore applications. With increase in size of wind turbines, the associated challenges in modelling aerodynamics, hydrodynamics, etc., are also bound to increase.

FOWTs are exposed to multi-hazard scenario of wind and wave conditions, which are simultaneous in nature. Schematic representation of components of FOWT and their interaction dynamics has been illustrated in Fig. 1. To assess their combined effect on the FOWT and to achieve the safety and stability of the supporting structure of FOWT, there is a need to investigate numerous complex loading conditions, viz, wind-induced aerodynamic loads, wave-induced hydrodynamic loads, dynamics of supporting structure, etc. International Electrotechnical Commission (IEC) standards enlists numerous design situations or Design Load Cases (DLC) to be considered towards evaluation of ultimate and fatigue loads on the FOWT during the design[3,4]. Tools of varying fidelity are adopted to assess the loads and responses of FOWTs under such challenging design situations.

For aerodynamics, Blade Element Momentum theory (BEM), Free Vortex Wake (FVW) and Computational Fluid Dynamics (CFD) are used, with the aforementioned approaches listed in the order of

*Corresponding author: (E-mail: keerthana@serc.res.in)

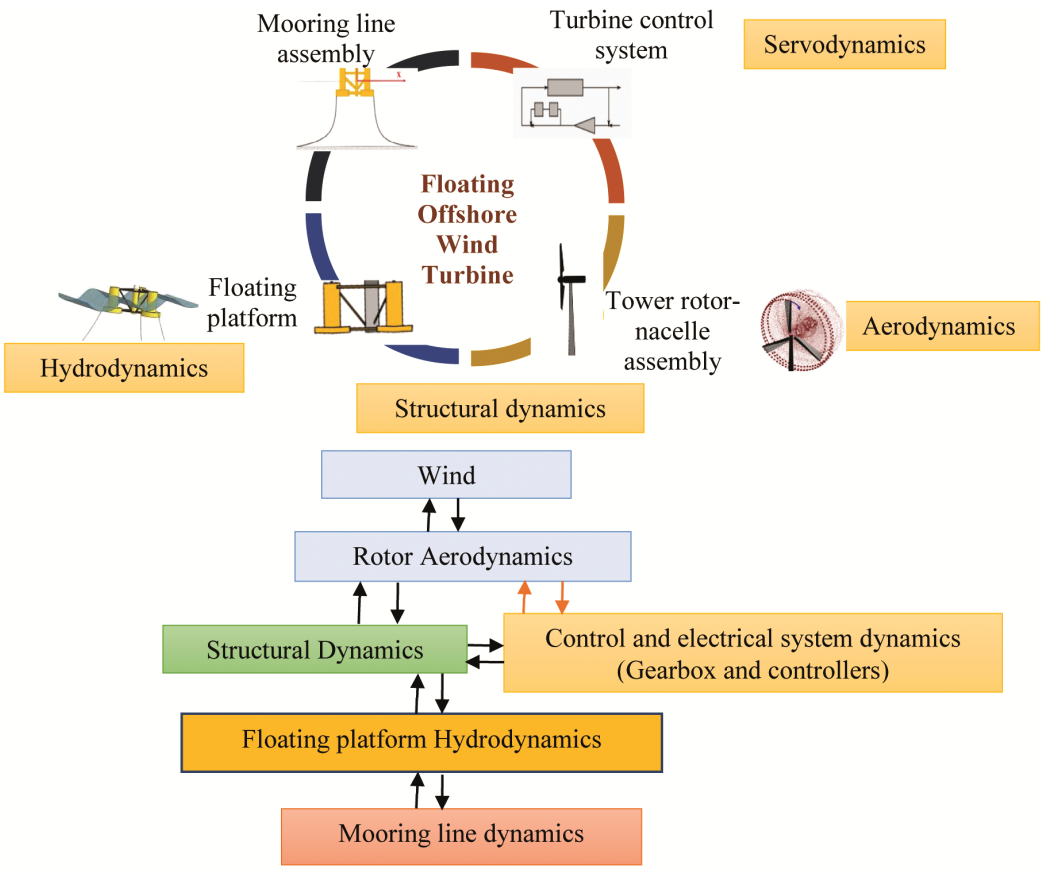

Fig. 1 — Schematic representation of FOWT components and the interaction dynamics.

increasing fidelity[5]. Similarly, for hydrodynamics, Morison equation, Potential flow theory, a hybrid approach of Morison equation and potential flow theory and CFD are used[6].

Though CFD is a tool of highest fidelity among other modelling tools/approaches, the computational intensive simulations makes it non-feasible to be applied for large number of DLCs that needs to be simulated, as prescribed by the IEC code. Hence, non-linear time domain analysis with low-medium fidelity tools are performed for preliminary design of structure including tower and floating platform as reported. Jonkman & Matha[7] presented dynamic response analysis of NREL 5MW turbine supportedon three types of floating platform concepts, viz, tension leg platform, spar buoy and barge, based on fully coupled non-linear time domain analysis using OpenFAST. All the floating platform concepts vary from each other based on the mechanism of stabilisation or source of restoring moments. The effect of duration of simulation on loads were also studied. The ultimate loads and response of NREL 5 MW wind turbine supported on monopile has been systematically analysed by Morató *et al.*[8] based on OpenFAST. Other studies with varying scope on NREL 5MW turbine supported on OC4 semisubmersible have been carried out[9-11]. Niranjan & Ramisetti[12] have carried out similar analysis of IEA 15 MWwind turbine supportedon Volturn US-S semi-submersible platform. In addition to insights on various design load cases, full-system linearization analysis towards identification of system frequencies was also presented.

Based on review of literature and from tabulated data on commonly adopted floating platforms for FOWT[2], it has been observed that most of the FOWTs adopt semi-submersible platforms. The present study involves numerous non-linear time domain simulations carried out towards assessment of the design loads of FOWT, with NREL 5 MW Reference Wind Turbine (RWT) supportedon OC4 DeepCwind semi-submersible under operating conditions and parked condition. Comprehensive time-domain analysis of aforementioned configuration, covering various DLCs has not been reported elsewhere to the author's knowledge. The scope of the paper is

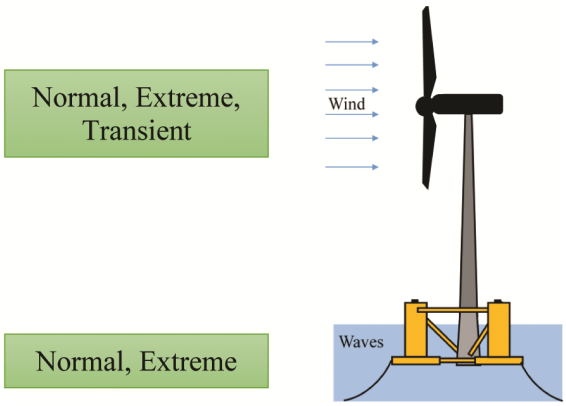

Fig. 2 — Scope of present study.

schematically presented in Fig. 2. The effect of normal, extreme and transient conditions for wind loading and normal and extreme conditions for wave loading have been considered, in suitable combination prescribed by IEC standard. This accounts for the effect of multiple hazards on FOWT. The coupled non-linear time domain analysis has been carried out using OpenFAST tool developed by National Renewable Energy Laboratories (NREL). It is a comprehensive aero-hydro-servo-elastic simulation tool with integrated models for multiple-physics, viz, wind inflow, aerodynamics, hydrodynamics, controller (servo) dynamics and structural dynamics. The scope of the paper does not include DLCs involving occurrence of faults. The loads and responses evaluated based on the numerical simulations with consideration of environment (wind and wave)-structure interaction will be immensely useful towards the design on structure including rotor-nacelle assembly, tower and floating platform. Such assessment of ultimate and fatigue loads acting on FOWT from coupled analysis ensures safety of FOWT during its design life.

2 Materials and Methods

In the present study, NREL 5 MW Reference Wind Turbine (RWT)[13] supported on OC4 DeepCwind semi-submersible[11] has been considered. It is a three-bladed upwind turbine with rotor diameter of 126 m and hub diameter of 3 m. Blades consists of a cylindrical segment close to the root to enable connection to the hub. DU and NACA64 series of airfoils are used along the length of blade with higher chord length and twist close to the root and lesser chord length with zero twist close to the tip. The characteristics of turbine have been presented in Table 1. The characteristics of floating platform are

Table 1 — Properties of NREL 5MW turbine[13].

Parameter	Value
Rated power	5 MW
Rotor orientation, configuration	Upwind, 3 blades
Cut-in (V_{in}), rated (V_r) and cut-out (V_{out}) wind speed	3 m/s, 11.4 m/s and 25 m/s
Cut-in, rated rotor speed	6.9 rpm, 12.1 rpm
Rated tip speed	80 m/s
Rotor mass, nacelle mass, tower mass	110 tonne, 240 tonne, 347.5 tonne
Drive train	High speed, multiple stage gearbox
Controllers	Variable speed, collective pitch
Hub height	90 m above Mean Sea Level (MSL)
Water level	200 m above seabed

Table 2 — Properties of mooring line.

Parameter	Value
Depth to anchor and Depth to fairlead	200 m and 14 m
Radius to anchor and Radius to fairlead	837.6 m and 40.868 m
Unstretched mooring line length	835.5
Mooring line diameter	0.766

available in literature[11]. The tower supporting the rotor-nacelle assembly is a tapered cylindrical tower with base diameter of 6 m and top diameter of 3.87 m. The supporting tower is connected to the central column of OC4 DeepCwind semi-submersible. This floating platform has three main offset columns and a central column, with a number of diagonal cross and horizontal bracing components. It is hybrid type floating platform with restoring moment from buoyancy and mooring. For the station keeping and stability of the floating platform, three numbers of catenary mooring lines are used. The mooring lines are oriented at 60°, 180° and 300° about the vertical axis. The properties of mooring line are presented in Table 2.

2.1 Environmental loads

The wind and wave conditions for operating and parked condition of the FOWT, as prescribed by IEC standard in the form of Design Load Cases (DLCs) have been enlisted in Table 3. For DLCs 1.1, 1.3, 1.4, 1.5 and 1.6, the turbine is operational and produces power in the wind speeds ranging from cut-in to cut-out wind speed. The corresponding wave parameters, *viz*, significant wave height and peak spectral period Table 4 for normal and severe sea states are obtained from a metocean data available in literature[8].

Table 3 — Wind and wave conditions considered for the study.

Turbine state	DLC	Wind speed	Wind model	Wave model
Power production / Operating condition	1.1	Wind speed: 3 m/s (V_{in}) to 25 m/s (V_{out}) at interval of 2 m/s	NTM	NSS
	1.3	Wind speed: 3 m/s (V_{in}) to 25 m/s (V_{out}) at interval of 2 m/s	ETM	NSS
	1.4	Around rated wind speed: ECD $\pm V_r \pm 2$	ECD	NSS
	1.5	Wind speed: 3 m/s (V_{in}) to 25 m/s (V_{out}) at interval of 2 m/s with vertical and horizontal shear	EWS	NSS
	1.6	Wind speed: 3 m/s (V_{in}) to 25 m/s (V_{out}) at interval of 2 m/s	NTM	SSS
Parked/Idling condition	6.1	0.95 x 50-year wind speed (V_{50})	EWM	ESS

DLC-Design Load Case; ECD-Extreme Coherent gust with direction Change;
ESS-Extreme Sea State; ETM-Extreme Turbulence Model; EWM-Extreme Wind Model; EWS- Extreme Wind Shear; NSS-Normal Sea State; NTM-Normal Turbulence Model; SSS-Severe Sea State

The average wind speed and turbulence characteristics about the rotor plane is important towards evaluation of the aerodynamic loads on blades and tower. The wind field around the rotor has been generated using Turb Simstochastic inflow generator of OpenFAST. A uniformly spaced grid with 31 x 31 points covering an area slightly beyond the rotor plane area of 145 m x 145 m has been used. Power law based variation of wind field along the height of the structure, with power law coefficient of 0.14 has been considered for turbulent inflow wind generation, as corresponding to Class B wind turbine. Though a smoother and less turbulent wind characteristics are expected in offshore conditions, the value of power law coefficient has not been reduced in line with other literature on the subject.

For DLC 1.1 and 1.3, IEC Kaimal spectra with exponential coherence based Normal Turbulence Model (NTM) and Extreme Turbulence Model (ETM) were used, respectively. The spectra with coherence functions in frequency domain is converted to 3-components of wind speed vectors across the rotor plane through Inverse Fourier Transform. Random seed variation for DLCs has been achieved by varying random number generator usedfor generation of stochastic wind field in TurbSim and wave generation in HydroDyn. For DLCs 1.3 and 1.4, the transient wind events like gust, direction change and shear have been generated using IECWind tool of NREL. JONSWAP spectrum has been used for modelling stochastic waves for all considered sea states, including normal, severe and extreme sea states. The spectral model requires input on significant wave height and spectral period. This information is conditioned based on the wind speed as provided in Table 4.

Table 4 — Wave parameters considered for simulations.

Wind speed (m/s)	Significant Wave Height (m)		Peak Spectral Period (s)	
	NSS	SSS	NSS	SSS
4.00	1.10	6.3	8.52	11.5
6.00	1.18	8.0	8.31	12.7
8.00	1.32	8.0	8.01	12.7
10.00	1.54	8.1	7.65	12.8
12.00	1.84	8.5	7.44	13.1
14.00	2.19	8.5	7.46	13.1
16.00	2.60	9.8	7.64	14.1
18.00	3.06	9.8	8.05	14.1
20.00	3.62	9.8	8.52	14.1
22.00	4.03	9.8	8.99	14.1
24.00	4.52	9.8	9.45	14.1

2.2 Aerodynamic modelling

The aerodynamic loads acting on the rotor have been evaluated based on Blade Element Momentum (BEM) theory by AeroDyn module of OpenFAST. BEM theory was developed based on 1D-momentum theory (by considering conservation of momentum in a control volume) and 2D-blade element theory. Momentum theory considers the rotor as a friction less permeable actuator disc, that does not impart any rotational velocity to the flow. The control volume that surrounds the actuator disc is assumed to be bound by a stream tube, with two cross-sections upstream and two cross-sections downstream as shown in Fig. 3a.

The actuator disc removes energy from the stream tube through a drag force that causes a pressure drop in the fluid downstream of the disc. The axial induction factor (a), defined as the fractional reduction in flow speed between free stream and actuator disc is given by

$$U_1 = U(1-2a) \quad \ldots(1)$$

where U is the free stream velocity and U_1 is downstream flow velocity. The flow speed at the disc is given by

$$u_{disc} = U(1-a) \quad \ldots(2)$$

For the model to account for rotational effects, the stream-tube is divided into annular sections with local radius,r, thickness, dr, resulting in area of annulus as $2\pi\, r\, dr$. It is considered to be rotating with a speed of Ω. The increase in rotational flow downstream is considered to be ω. Based on the conservation of momentum, the axial force $dF_{A1}$and torque on rotor annulus are given by

$$dF_{A1} = 2\pi\, r\, \frac{1}{2}\rho\, U^2\, 4a\,(1-a)dr \quad \ldots(3)$$

$$dF_{T1} = 4b\,(1-a)\rho U\, \Omega r^2\, \pi\, r\, dr\,(1-a) \quad \ldots(4)$$

Where b is angular or tangential induction factor given by

$$b = \frac{\omega}{2\,\Omega} \quad \ldots(5)$$

Detailed equations and derivations are available elsewhere[14]. Thus, the axial force and torque of the annulus of rotor shall be determined upon knowing axial and tangential induction factors. Owing to the fact that the induction factors are not known, momentum theory cannot be used directly for evaluation of aerodynamic loads. Blade element theory is needed to get the axial and thrust forces.

Blade element theory assumes the rotor blades to be divided into small discrete elements, that act as 2-D airfoils without depending on the surrounding elements. Hence, the aerodynamic loads on the blades are assumed to be dependent on lift and drag characteristics of the considered airfoil shapes. The axial thrust dF_{A2} and torque dT_2 are evaluated by resolving the lift and drag forces, written in terms of lift $C_L$and drag $C_D$coefficients as given below.

$$dF_{A2} = N\, \frac{1}{2}\rho\, V^2\, c\,(C_L cos\phi + C_D sin\phi)\, dr \quad \ldots(6)$$

$$dT_2 = N\, \frac{1}{2}\rho\, V^2\, c\, r\,(C_L sin\phi - C_D cos\phi)\, dr \quad \ldots(7)$$

where N is the number of blades. From Fig. 3b showing the velocity triangle of forces in the airfoil section, the angle of attack (ϕ) is obtained as

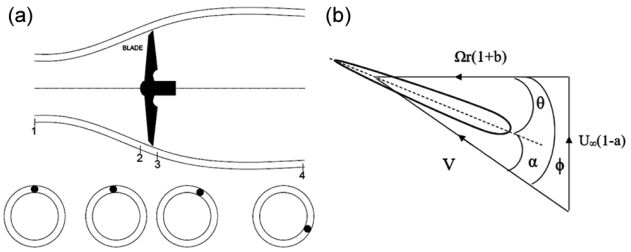

Fig. 3 — (a) Stream tube concept for BEM and (b) velocity triangle.

$$\phi = \tan^{-1}\left(\frac{U\,(1-a)}{r\,\Omega\,(1+b)}\right) = \tan^{-1}\left(\frac{(1-a)}{\lambda\,(1+b)}\right) \quad \ldots(8)$$

where λ is the non-dimensional local speed ratio.

$$\lambda = \frac{r\omega}{U} \quad \ldots(9)$$

The resultant fluid flow velocity is given by

$$V = [(r\,\Omega(1+b))^2 + (U\,(1-a))^2]^{1/2} = U[(\lambda\,(1+b))^2 + (1-a)^2]^{1/2} \quad \ldots(10)$$

Certain underlying assumptions in BEM have been observed to be inapplicable during platform motion, where platform motion results in wind turbine rotor subjected to various wake stages and non-axial flow conditions[7]. Engineering models derived based on experiments and tools of higher fidelity overcome some of the inherent limitations of BEM approach. In the present study, Beddoes-Leishman unsteady model is used to account for unsteady airfoil aerodynamics, Prandtl model to account for tip loss and hub loss and Pitt-Peters model skewed wake model for skewed wake effects. The thrust and power output from the turbine evaluated using BEM approach with engineering correction models have been reported to be comparable with tools of higher-fidelity[5].

2.3 Hydrodynamic modelling

For modelling hydrodynamic loading on the floating platform, potential flow theory/diffraction theory is considered in the HydroDyn module of OpenFAST. It is used when the characteristic dimension of floating platform is significantly higher than compared to wave length. The fluid is assumed to be inviscid, irrotational and incompressible. In OpenFAST framework, the hydrodynamic parameters are computed in frequency domain using WAMIT module and then converted to time-domain parameters. These parameters serve as boundary conditions to compute hydrodynamic loads and responses for coupled simulations of FOWT. The total velocity potential is obtained from incident,

diffraction and radiation potentials. The diffraction and radiation potentials at every node is obtained from boundary element method. The wave force on the structure is calculated using linear Bernoulli equation.

For members with smaller diameter/size, Morison equation as given below is used to calculate the wave loading.

$$F_T = \frac{\pi D^2}{4}\rho C_{Mw}\dot{u} + \frac{1}{2}\rho C_{Dw} D u|u| \quad \ldots(11)$$

Where F_T is the total wave force, C_{Dw} and C_{Mw} are the drag and inertia coefficients, u and $\dot{u}$ are the water particle velocity and acceleration, D is the diameter of the structure and ρ is the density of water. The first term in the equation is the inertia component and the second term is the drag component. Such medium-fidelity tools for hydrodynamic modeling have been reported to under predict the responses of floating platform[15,16]. It is noteworthy that all the parts/components of OC4 DeepCwind floating platform is cylindrical in shape. This eases the application of viscous effects for potential flow based hydrodynamic analysis tools.

2.4 Mooring dynamics modelling

The mooring system model in the MoorDyn model of OpenFAST is based on lumped mass method. Each of the three mooring lines have been divided into a number of segments (i) and nodes ($i+1$). The nodes are connected by equivalent spring-damping system. The differential equations representing dynamic equilibrium and continuity of each node is solved to evaluate the mooring line restoring forces. The nodes are subjected to gravity, tension and fluid force, while the spring-damping system is not subjected to any loading. Morison equation is used to calculate drag and added mass of the mooring line. This approach is widely used owing to its simplistic nature[7].

2.5 Simulation settings

For the variable speed and pitch control, control system developed specifically for 5MW wind turbine is used as a Dynamic Linked Library (DLL) by ServoDyn module of OpenFAST. Variable speed controller is engaged below rated wind speed, to maximise power generation at lower wind speeds. Pitch controller is used to increase the blade twist with increase in wind speed, thereby reducing the projected area of the blade. This aids in maintaining rated power from rated wind speed to cut-out wind speed and regulate the loads on the turbine supporting structure. OpenFAST couples multiple-physics as explained in preceding sections in a unified framework and solves Kane's equation of motion for multi-body systems by numerical integration to evaluate loads and responses of FOWT.

The degrees of freedom (DOF) considered for the equation of motion include, first and second flapwise blade modes (6 numbers), first edgewise blade mode (3 numbers), generator DOF, yaw DOF, drivetrain torsion DOF, first and second fore-aft bending mode DOF, first and second tower side-to-side bending DOF, floating platform surge, heave, sway, roll, pitch and yaw DOF. These sums up to a total of 22 DOFs. The co-ordinate systems and terminologies have been represented in Fig. 4.

The duration of simulation as prescribed by the IEC code for each of the DLCs has been increased by 100 s to account for initial transient in the time domain simulations. For transient wind event cases, viz, DLC 1.3 and 1.4, the event has been initiated after 100 s to assess the effect of the events beyond the time period of occurrence of numerical transients. Number of coupled non-linear time domain simulations performed for each DLC has been presented in Table 5. A time step size of 0.02 s has been used for all the simulations.

3 Results and Discussion

Among three components of forces and moments (co-ordinate system presented in Fig. 4), tower axial force (F_z) and tower base fore-aft moment/overturning moment/pitching moment (M_y) are significant, respectively. Similarly, the blade root flapwise (out-of-plane) and edgewise (in-plane) moments are significant and govern the design of rotor-nacelle assembly. The discussions on interaction of environmental loads, viz, wind and wave with FOWT will be made with the aid of aforementioned parameters.

3.1 Validation

The results of time-domain simulations have been initially validated with literature. For fixed base turbine configuration (without the floating platform), simulations corresponding to DLC 1.1 have been carried out for wind speeds between cut-in and cut-out wind speeds with turbulent wind characteristics. For every wind speed, the mean, maximum and minimum values of loads and responses have been obtained from the simulations. The tower base fore-

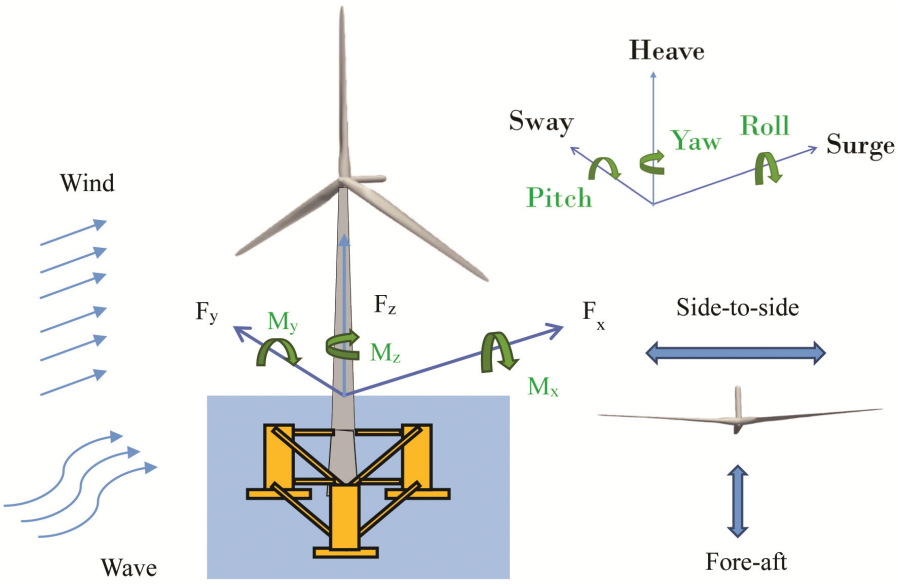

Fig. 4 — Co-ordinate system for forces / moments.

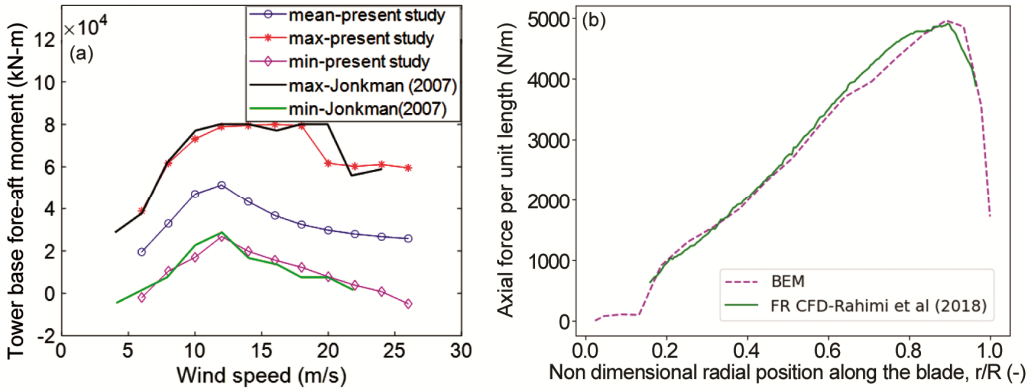

Fig. 5 — (a) Comparison of tower base fore-aft moment and (b) Comparison of axial force per unit length of blade with literature

Table 5 — Number of simulations for each DLC.

DLC	Wind/wave combination	Random seeds	Yaw misalignment angles	Wind type	Initial Azimuth	Duration of simulation(s)	Total number of simulations
1.1	11	20	3	1	1	700	660
1.3	11	6	3	1	1	700	198
1.4	1	-	3	6	4	160	72
1.5	11	-	3	4	4	230	528
1.6	11	6	3	1	1	3700	198
6.1	3 (wind-wave misalignment)	6	3	1	1	3700	54

aft moment has been compared with OpenFAST based results under identical conditions in Fig. 5a. A good comparison of the tower base fore-aft moments are indicative of the correctness of the simulation framework.

Similarly, the axial force per unit length of blade obtained from the present study have been validated against with blade-resolved/fully resolved CFD simulations for steady inflow case at a wind speed of 9 m/s[18] as shown in Fig. 5b. The axial force per unit length of the blade of 5MW turbine at 9 m/s from BEM based simulations of OpenFAST compares well with blade-resolved CFD simulations. This comparison aids in gaining confidence on the aerodynamic loads evaluated using BEM. However, similar comparison under turbulent inflow

could not be made due to non-availability of data in literature.

3.2 Design load case 1.1

For each wind speed and sea state combination, a number of simulations need to be carried out (Table 5) to obtain a reliable long term probability distribution of extreme values[3,4]. This ensures achieving characteristic load effect on FOWT for 50-year return period through a statistical extrapolation technique. A total of 11 numbers of wind and wave combination for Normal Sea State (NSS) as per Table 4 have been considered. For every combination, twenty random seeds and three yaw misalignment angles of 0°, +8° and -8° have been considered. The time history of wind speed, wave elevation, blade root moments and tower base fore-aft moment for wind speed of 12m/s has been presented in Fig. 6. The blade root flapwise/out-of-plane moments have been observed to be sensitive to stochastic variation in wind speed compared to the blade root edgewise moment. The trend in variation of tower base fore-aft moment following wind speed variations is indicative that DLC 1.1 dominated by wind load, compared to wave load.

For each of the simulations, mean, maximum and minimum values of forces, moments and responses have been evaluated from the corresponding time history, beyond the initial transient portion. The mean, maximum and minimum values for each wind speed bin have been obtained by averaging the corresponding parameters of over simulations with multiple random seeds. The variation of mean values of power output and rotor thrust have been presented in Fig. 7. The turbine reaches rated capacity of 5 MW near the rated wind speed of 11.4 m/s, beyond which the power generation is maintained up until cut-out wind speed.

Fig. 8 shows the variation of mean, minimum and maximum values of tower axial force (F_z) and tower base fore-aft moment (M_y) with wind speed. Though

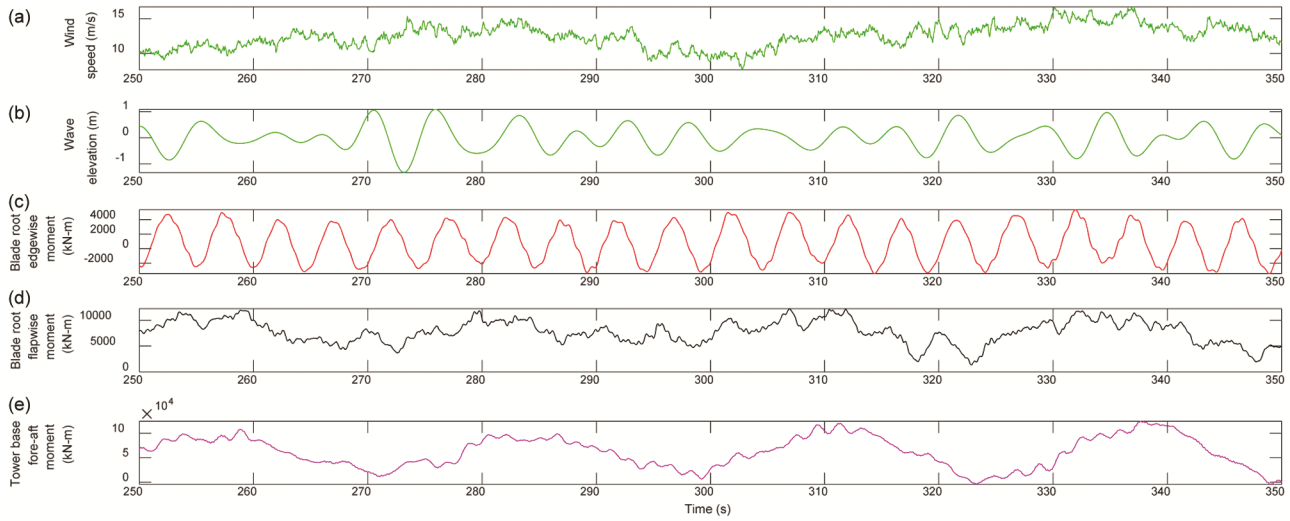

Fig. 6 — Time-series of different output parameters from DLC 1.1 at wind speed of 12 m/s (a) Wind speed, (b) Wave elevation, (c) Blade root edgewise moment, (d) Blade root flapwise moment and (e) Tower base fore-aft moment.

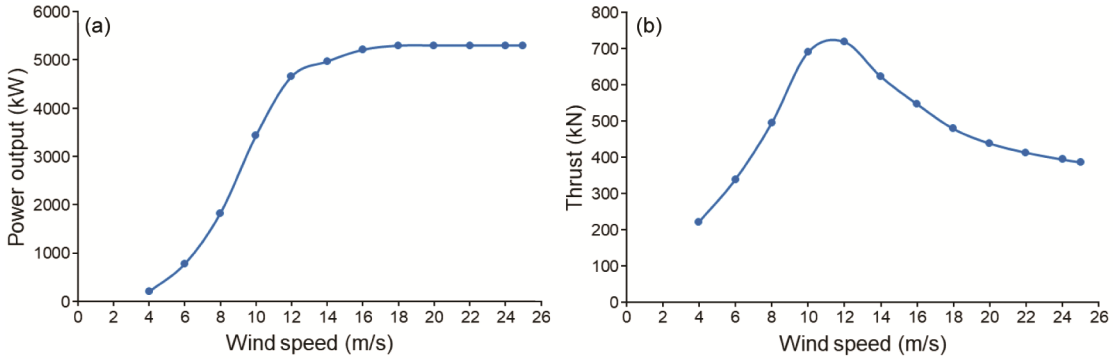

Fig. 7 — Variation of (a) power output and (b) rotor thrust with wind speed.

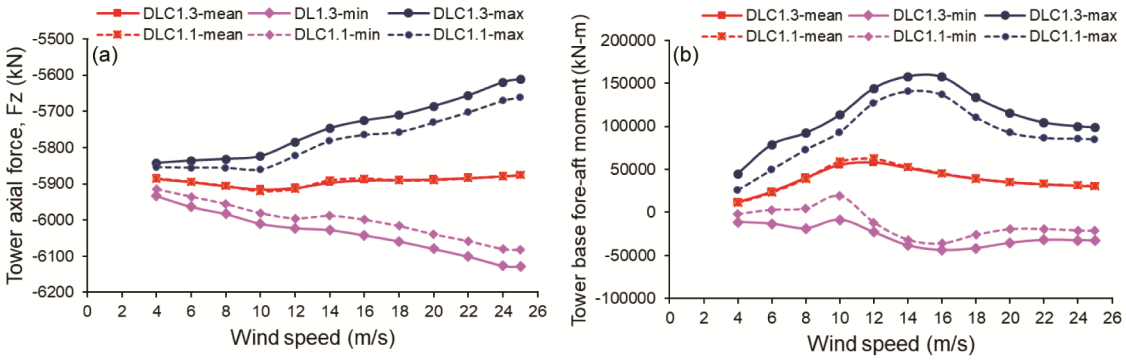

Fig. 8 — (a) Tower axial force and (b) Tower base fore-aft moment for DLC 1.1 and 1.3.

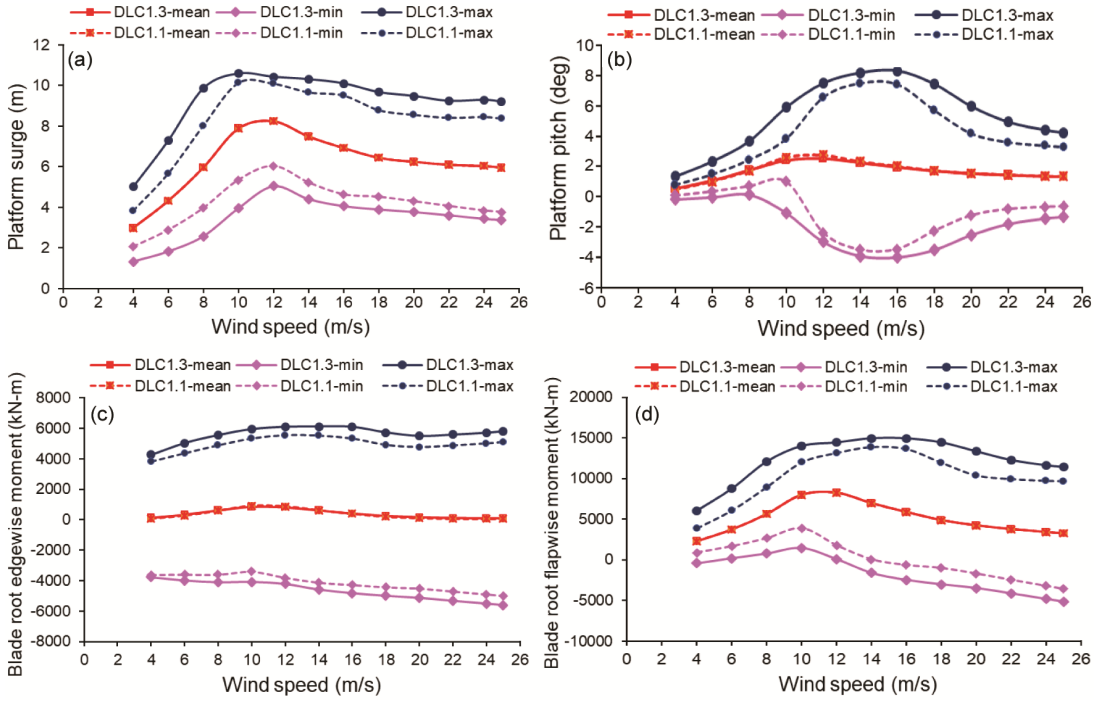

Fig. 9 — Platform (a) surge motion, (b) pitch motion, (c) blade root edgewise moment and (d) blade root flapwise moment for DLC 1.1 and 1.3.

wave loading is also considered, all further plots will be presented in terms of wind speed for simplicity. The trend in variation of tower axial force steadily increases with wind speed. The shaft tilt of the turbine is designed such that the supporting tower is predominantly loaded in its axial plane. Thrust force increases rated wind speed, beyond which it exhibits reducing trend owing to the fact that pitch controller of the turbine is engaged after rated wind speed, as mentioned earlier. Similar trend of higher loads around the rated wind speed have been reported for pitch controlled turbines[8,19]. The tower base fore-aft moments have been observed to be higher from rated wind speed to wind speed of 16 m/s.

Since the tower is connected to the central column of the floating platform, the variation of tower base fore-aft moment is reflected in the platform movements, viz, surge and pitch as shown in Fig. 9. The blade root edgewise moment remains almost constant wind speed, whereas the blade root flapwise moment varies with wind speed, since it is caused by out-of-plane forces.

Statistical extrapolation approach is required on the loads from DLC 1.1 to obtain characteristic loads for 50-year return period. The samples of tower fore-aft moment, blade root flapwise and from various wind speed bins have been arranged in ascending order. This data is fitted with Gumbel distribution, using a

least square fitting as shown in Fig. 10. The green line indicates Gumbel fit of the data with 95% confidence interval.

The Gumbel fit is extrapolated to obtain characteristic load for probability of exceedance (POE) corresponding to 50-year return period. The POE for 50-year return period is 3.8×10^{-7}, based on inverse of return period. The extrapolated value of tower base fore-aft moment has been obtained as 154643kN-m. The extrapolated loads obtained by this approach is also needed towards calibration of the results from DLC 1.3. In case of the loads obtained from DLC 1.3 being less than that extrapolated from DLC 1.1, the parameter 'c' required for generation of ETM based wind field for DLC 1.3 needs to be increased.

Further, a comparison of tower axial force and tower base fore-aft moment for FOWT has been made with that of an equivalent fixed base wind turbine subjected to similar wind conditions in Fig. 11. For the latter case, it is to be noted that the floating platform and wave loading are absent.

The tower axial forces are comparable between land based bottom-fixed turbine and floating offshore wind turbine, with marginally lesser forces for floating case. In case of tower fore-aft moment, the maximum and minimum values for FOWT are significantly higher than that of bottom-fixed turbine, though the mean loading has been observed to be of comparable magnitudes.

3.3 Design load case 1.3

The key difference between DLC 1.1 and 1.3 is that for DLC 1.3, Extreme Turbulence Model (ETM) is used instead of Normal Turbulence Model (NTM). The case does not mandate statistical extrapolation for characteristic loads and hence, the number of random seeds for the simulations have been limited to six. Since the trend in quantities of interest of the present study for DLC 1.1 and 1.3 have been observed to be similar, they have been plotted together in Fig. 11. The maximum values of tower base fore-aft moment and blade root flapwise moment have been observed at wind speeds of 16 m/s and 18 m/s, rather at rated wind speed observed for DLC 1.1. Similar behaviour for monopole supported 5MW offshore wind turbine has been reported[18] and attributed to turbulent fluctuations causing trough in blade pitch. Reduction in blade pitch at higher wind speeds of 16 m/s to 18

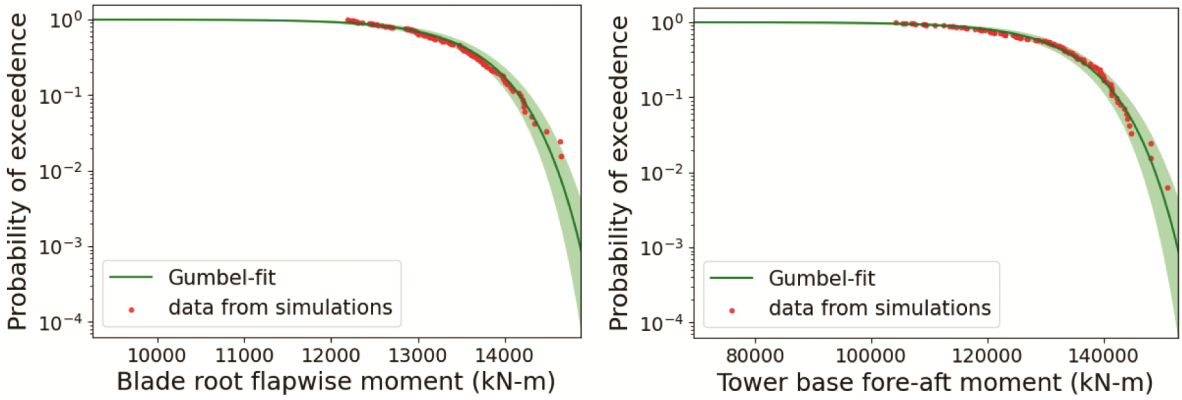

Fig. 10 — Fitting of Gumbel distribution to (a) blade root flapwise moment and (b) tower base fore-aft moment.

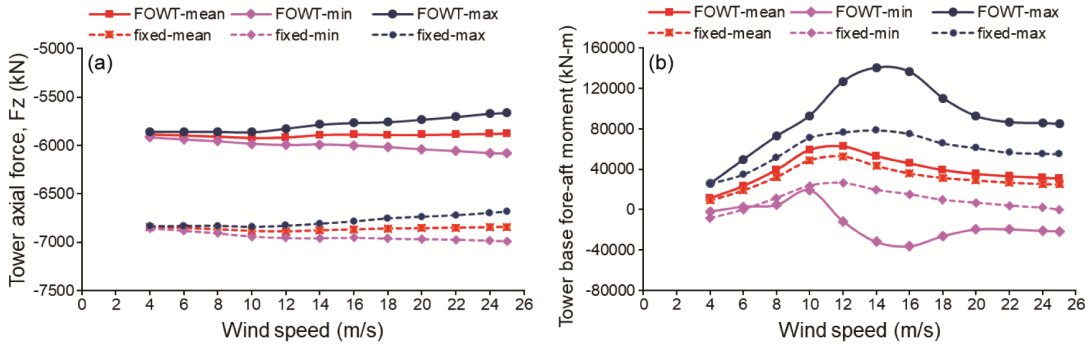

Fig. 11 — Comparison of (a) tower axial force and (b) tower base fore-aft moment for fixed-bottom and floating offshore wind turbine for DLC 1.1.

m/s results in increased loading due to increased exposed area of the blade. The maximum value of tower base fore-aft moment obtained from DLC 1.3 of 157982 kN-m is higher than the extrapolated value of 154643 kN-m from DLC 1.1. The variation of the parameter 'c' used for generation of wind field based on ETM has not been modified.

3.4 Design load case 1.4

The effect of discrete wind event like gust and rapid change in wind direction during normal operation of the considered FOWT have been studied.

For certain configurations of FOWT, DLC 1.4 has been reported in literature to produce design-driving ultimate blade and shaft loads. It is hence one of the potentially critical events during normal operation. The normal sea state has been considered for these cases with no variation in random seed. For DLC 1.4, the effect of Extreme Coherent gust with Direction change (ECD) for six cases (ECD±R±2.0) around rated wind speed (R) of 11.4 m/s, three yaw misalignment angles of -8°, 0° and +8° and four initial blade azimuth angles of 0°, 30°, 60° and 90° have been investigated.

The occurrence of gust over short duration of about 10 seconds and extreme wind direction in the range of -65° to +65° as shown in Fig. 12 (for two typical cases) influences the loads on FOWT depending on initial azimuthal position of the blade. The effect of direction change is evident from significant increase/decrease in y component of velocity (V_y) in the plots. This DLC aids in gaining understanding of the correlation between initial azimuth angle, yaw misalignment and the tower base fore-aft moment. It can be observed from Fig. 13 that initial azimuth angle of the blade has less significant effect on the fore-aft moment compared to the yaw misalignment. The maximum blade root flapwise moment has been observed to be 20845 kN-m for the case of ECD-R+2.0 for yaw misalignment of -8° and blade azimuth of 90°. The maximum tower base fore-aft moment has been observed to be 148706 kN-m. Below rated wind speed, loads are higher for rotor with yaw misalignment. It has been inferred that yaw misalignment affects the loads than initial azimuth angle of blades.

3.5 Design load case 1.5

For DLC 1.5, the effect of Extreme Wind Shear (EWS) in horizontal (H) and vertical (V) directions for various wind speeds in the range of 4 m/s to 24 m/s, for three yaw misalignment angles of -8°, 0° and +8° and four initial blade azimuth angles of 0°, 30°, 60° and 90° have been investigated. The variation of tower base fore-aft moment and blade root moments with initial blade azimuth and yaw misalignment has been presented in Fig. 14 & 15, respectively.

The maximum tower base fore-aft moment of 145044 kN-m has been observed at wind speed of 12 m/s near rated wind speed among all other wind speeds during normal operation of the turbine. The governing case is EWSH- for yaw angle of -8° and initial blade azimuth angle of 90°.

3.6 Design load case 1.6

For DLC 1.6, Severe Sea State (SSS) wave parameters have been used with stochastic wind field based on NTM. The duration of simulation is 3600 s. Variation of tower base fore-aft moment and blade root flapwise moment for DLC 1.6 has been presented in Fig. 16. The trend in variation of loads have been observed to follow DLC 1.1 and 1.3. The magnitudes of the loads are significantly higher due to

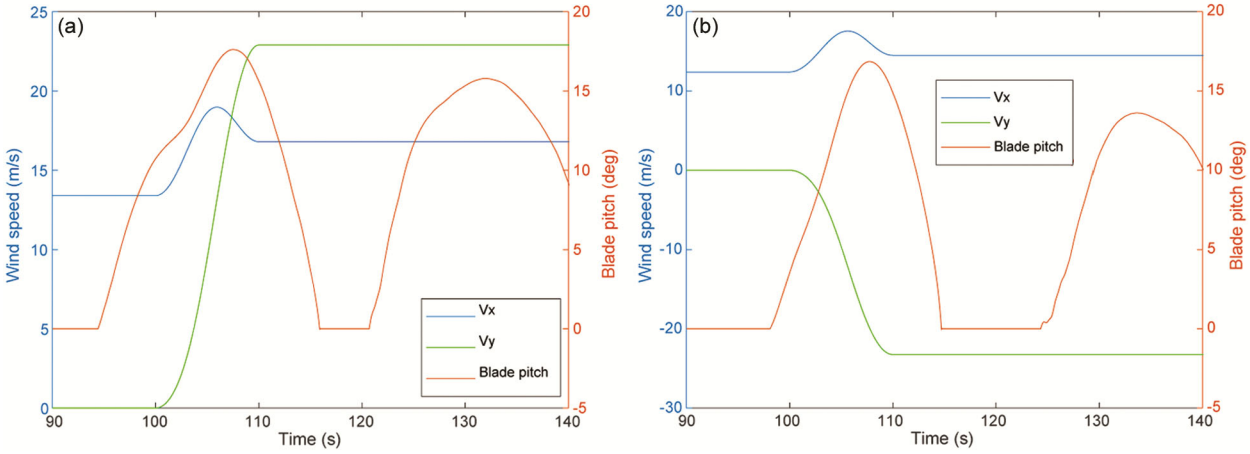

Fig. 12 — Effect of (a) wind speed and (b) direction change on blade pitch for DLC 1.4.

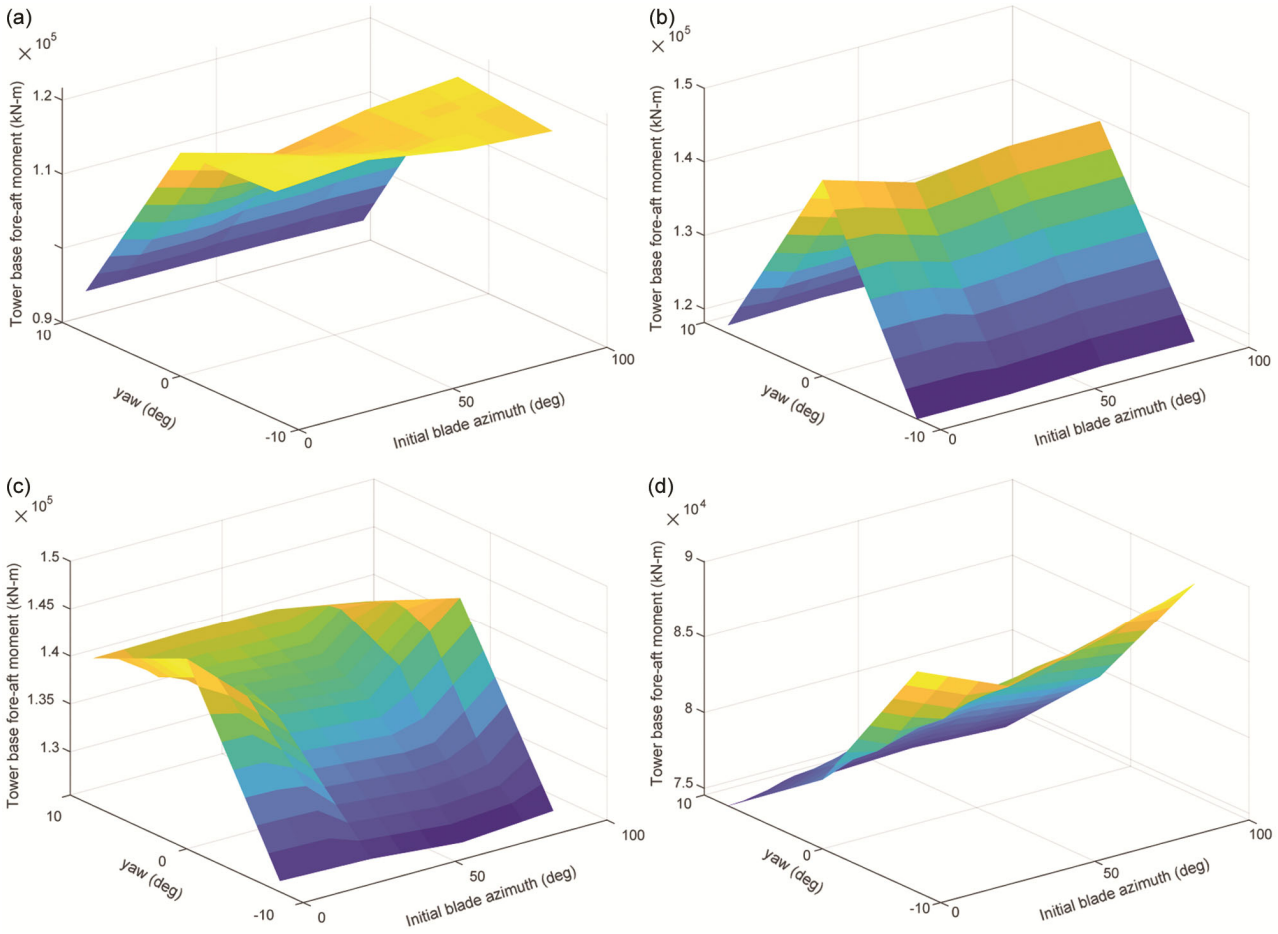

Fig. 13 — Variation of tower base fore-aft moment with azimuth and yaw for DLC 1.4.

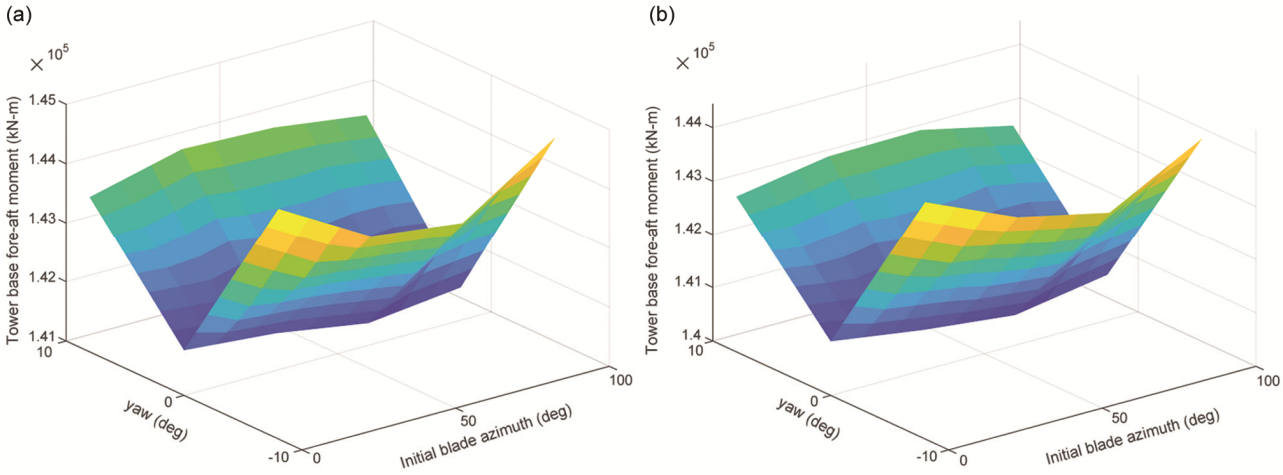

Fig. 14 — Variation of tower base fore-aft moment with azimuth and yaw for DLC 1.5.

conservative wave parameters considered for SSS. The maximum platform surge response has been observed to be 11.1 m, which is marginally higher than that observed in DLC 1.1 by about 5%. The maximum platform pitch response has been observed to be 10.3°, which is higher than that from DLC 1.1 by about 20%. The maximum value of tower base fore-aft moment has been observed to be 160458 kN-m. The highest tower base fore-aft/overturning moment is obtained from DLC 1.6.

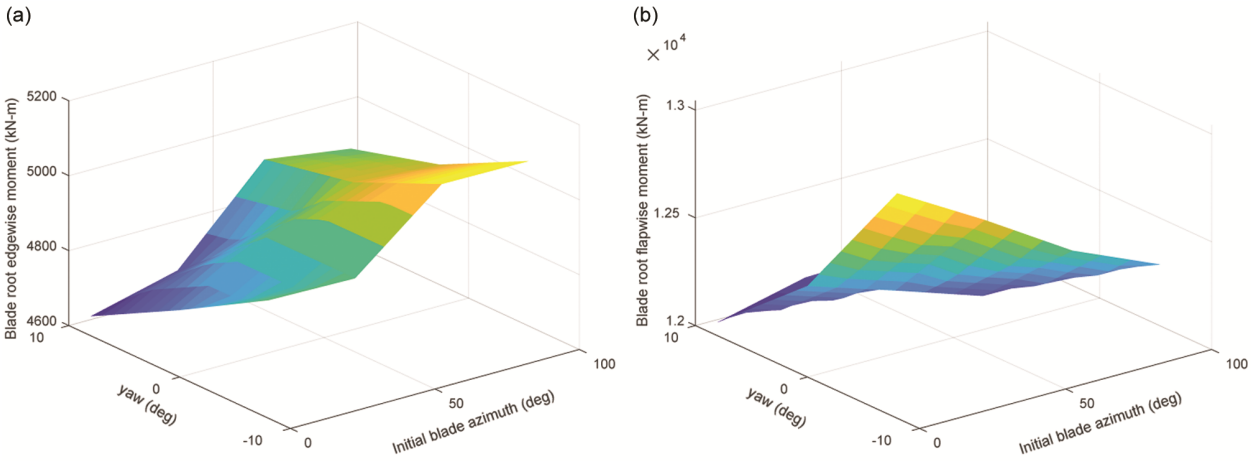

Fig. 15 — Variation of blade root moments with azimuth and yaw for DLC 1.5.

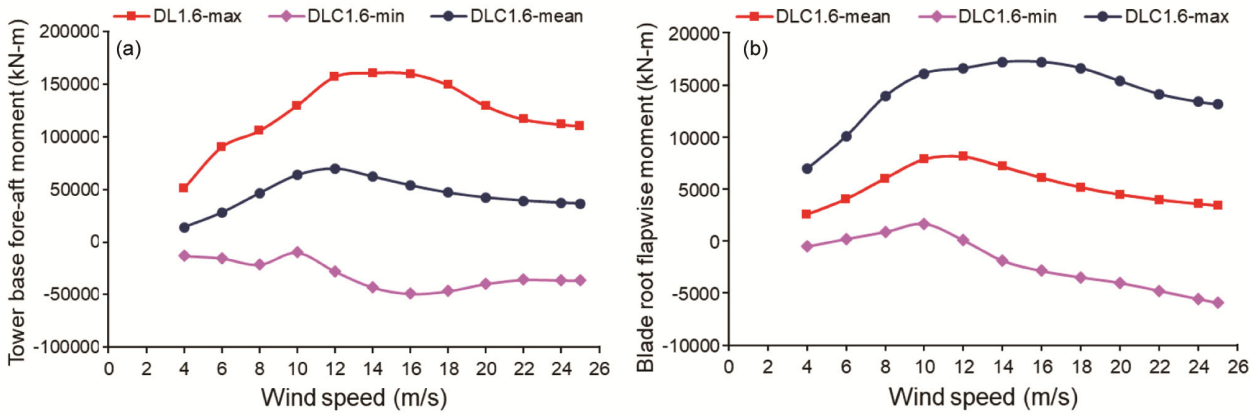

Fig. 16 — Variation of (a) tower base fore-aft moment and (b) blade root flapwise moment with wind speed for DLC 1.6.

3.7 Design load case 6.1

DLC 6.1 is a design situation in which the rotor is in parked condition. The rotor blades have been considered to be feathered, i.e., with blade pitch set to 90°. The controllers in ServoDyn module have been turned off. Owing to the parked condition of the rotor, the unsteady aerodynamics model and stall model have not been enabled. Wind-wave misalignment of ±30° have been considered in addition to 0° (aligned case), with six random seeds for each case as specified in Table 5. Wind speed of 47.5 m/s with Extreme Wind Model (EWM) and wave height and spectral period of 10.7 m and 14.2 s have been considered. The time history of wind speed, wave elevation, blade root moments and tower base fore-aft moment for wind-wave aligned case with yaw misalignment of +8° has been presented in Fig. 17.

It can be observed from the time series of the relevant parameters that the maximum value of tower base fore-aft moment occurs beyond 3300 s, when wave elevation is higher. The wind speed is significantly higher and they affect the blade root flapwise and edgewise moments. The frequency of oscillation of edgewise moment is higher than that of flapwise moment. The maximum value of tower base fore-aft moment has been observed to be 11207 kN-m.

3.8 Summary of all DLCs

For all the DLCs studied, the maximum values of tower base fore-aft moment and blade root moments have been presented in Table 6. The maximum tower base fore-aft moment has been observed to be 160458 kN-m. This corresponds to DLC 1.6 with normal wind and severe sea state conditions. However, the maximum values of blade root edgewise and flapwise moments of 8267 kN-m and 20845 kN-m, respectively have been observed from DLC 1.4 considering transient wind and normal sea state conditions. These characteristic loads need to be considered in conjunction with factor of safety (provided in Table 6) specified in IEC code.

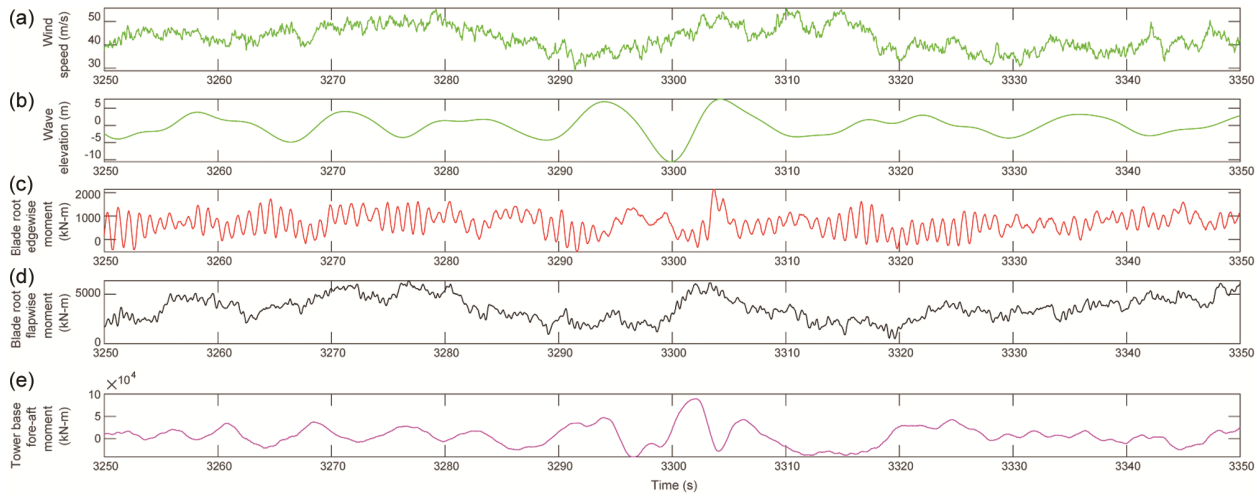

Fig. 17 — Time-series of different output parameters from DLC 6.1, yaw misalignment of +8° (a) Wind speed (b) Wave elevation (c) Blade root edgewise moment, (d) Blade root flapwise moment and (e) Tower base fore-aft moment.

Table 6 — Maximum loads from all the DLCs studied.

DLC	Tower base fore-aft moment (kN-m)	Blade root edgewise moment (kN-m)	Blade root flapwise moment (kN-m)	Partial safety factor
1.1	154643	6098	15278	1.25
1.3	157982	6121	14961	1.35
1.4	148706	8627	20845	1.35
1.5	145044	5633	13257	1.35
1.6	160458	6494	15256	1.35
6.1	111207	4164	11737	1.35

4 Conclusion

Numerical investigations on a configuration of FOWT with NREL 5MW turbine supported on OC4 semisubmersible floating platform has been carried out by considering normal, extreme and transient wind and wave exposure conditions. The key parameters that govern the design of rotor-nacelle assembly (RNA) and the supporting structure, viz, blade root flapwise and edgewise moments, tower fore-aft/overturning moment for various DLCs have been evaluated from the non-linear time domain analysis using OpenFAST. Five DLCs for turbine under normal operation and one DLC for turbine under parked condition has been considered. Wind gust with direction change (DLC 1.4) causes highest blade root flapwise and edgewise moments. The highest tower base fore-aft moment has been observed to be caused by severe sea state condition. The study highlights the importance of considering wind gusts and extreme wave events for the design on FOWT. The characteristic loads evaluated from the study, based on consideration of simultaneously occurring wind and wave events will aid in ensuring structural safety of FOWT during its design life. The results provide valuable information for further studies on optimising the design of FOWTs operating in harsh environmental conditions.

Acknowledgements

This paper is being published with the kind permission of the Director, CSIR-SERC. This paper has been assigned the registration number CSIR-SERC-1182/2024.The authors would like to thank the Council of Scientific and Industrial Research (CSIR), New Delhi, India for the financial support (Project No. MLP 209).The simulations were carried out in High Performance Computing (HPC) facility of CSIR-SERC.

References

1 International Energy Agency, Renewable Energy Market Update (2024).
2 Subbulakshmi A, Verma M, Keerthana M, Sasmal S & Harikrishna, P, *Renew Sustain Energy Rev*, 164 (2022) 112525.
3 61400-3-2, Wind Turbine Generator Systems, Part 3-2 – Design Requirements for Floating Offshore Wind Turbines (2019).
4 IEC 61400-3-1, Wind Turbine Generator Systems, Part 3-1 – Design Requirements for Fixed Offshore Wind Turbines (2019).

5 Burton T, Jenkins N, Sharpe D & Bossanyi E, Wind Energy Handbook (John Wiley & Sons, Chichester, West Sussex), 2nd Edn, ISBN: 9780470699751, 2011.

6 Chakrabarti S, Hydrodynamics of Offshore Structures (WIT Press, Southampton), ISBN: 978-0-90545-166-4, 1st Edn, 1987.

7 Matha D, Schlipf M, Cordle A, Pereira R & Jonkman J, Challenges in simulation of aerodynamics, hydrodynamics, and mooring-line dynamics of floating offshore wind turbines, *Proceedings of the International Offshore and Polar Engineering Conference*, Maui, United States, 2011.

8 Morató, Sriramula S, Krishnan N & Nichols J, *Renew Energy*, 101 (2017) 126.

9 Li L, Liu Y, Yuan Z & Gao Y,*Ocean Eng*,179 (2019) 92.

10 Li X, Zhu C, Fan Z, Chen X & Tan J,*Ocean Eng*, 199 (2020) 106960.

11 Robertson, A. et al, Offshore code comparison collaboration continuation within IEA wind task 30: Phase II results regarding a floating semisubmersible wind system, *Proceedings of the International Conference on Offshore Mechanics and Arctic Engineering*, San Francisco, United States, 2011.

12 Niranjan R & Ramisetti S B, *Ocean Eng*, 251 (2022) 111024.

13 Jonkman J, Butterfield S, Musial W & Scott G, *NREL/TP-500-38060*, 140 (2009).

14 MastersI, Chapman J C, Willis M R & Orme J A C, *J Mar Eng Technol*, 10 (2011), 25.

15 Hansen M O L, Sørensen J N, Voutsinas S, Sørensen N & Madsen H, *Prog. Aerosp. Sci*, 42 (2006) 285.

16 Behrens De Luna, R. et al,Comparison of different fidelity aerodynamic solvers on the IEA 10 MW turbine including novel tip extension geometries*, J Phys Conf Ser* 2265, Delft, Netherlands, 2022.

17 Jonkman J M, *NREL/TP-500-41958*, 68 (2007) 233.

18 Rahimi H, Martinez Garcia A, Stoevesandt B, Peinke J & Schepers G,*Wind Energy,* 21(2018) 618.

19 Rinker J et al,Comparison of loads from HAWC2 and OpenFAST for the IEA Wind 15 MW Reference Wind Turbine*, J Phys Conf Ser*, online, 2020.